Proceedings of the 17th World Congress
The International Federation of Automatic Control
Seoul, Korea, July 6-11, 2008

Design and Analysis of Switch Mode Amplifier for Actuator Array Using MIMO Optimal Feedback Quantization

Jwu-Sheng Hu* and Keng-Yuan Chen**

** Department of Electrical and Control Engineering,*
National Chiao Tung University, Hsinchu 300, Taiwan, ROC.
(Tel: 886-3-5712121 ext. 54318; e-mail: jshu@cn.nctu.edu.tw)
*** Department of Electrical and Control Engineering,*
National Chiao Tung University, Hsinchu 300, Taiwan, ROC.
(e-mail: bettery.ece94g@nctu.edu.tw)

Abstract: The system analysis of the MIMO optimal feedback quantization used to produce switching signals is proposed here. The switching signals are then fed into the switch mode power amplifier to drive actuator array. The architecture of the power amplifier used in this paper allows the sharing of switching elements among actuators and is different from the traditional one-to-one method in actuating a large number of devices. To actuate all of the devices at the same time, the MIMO optimal feedback quantization generates control signals optimally basing on minimizing the weighted measure of quantization error. The discussion on bounding the system states under the zero initial conditions is made. The result tells that the stability can be achieved by limiting the maximum amplitude of inputs when the MIMO system has stable zeros. To simplify the computational complexity of quantization, a sub-optimal method for actuating three-actuator system is mentioned. A design example of 2-input 2-output system which is applied to the class-D stereo audio amplifier (dual actuators) is addressed. The control performance and cross-talk behavior are investigated.

1. INTRODUCTION

There has been a growing need to achieve control objective using array of actuators. Examples include humanoid robots with a large number of motors [1], a variable shape of a reflective surface which can be applied to the projection display systems [2-3], the Virtual Audio Reality (VAR) that manipulate the spatial sound [4] and the Audio Spotlight that puts the sound where we want [5], etc. The easiest way to drive the array actuators is to have an independent amplifier for each actuator. However, for a large number of actuators, this 1-to-1 configuration might be inefficient and costly [6]. Although several types of amplifier topology were proposed in [4] [7], there are limitations of the type of input signals or actuators [6]. Another issue involved in array actuation is the power amplification method. Switch mode amplifiers are very common in 1-to-1 cases. The switching signal can be generated either by PWM or Sigma-Delta methods. But for array actuators using modified architecture, the switching signal for any one of the amplifiers cannot be independent to others because the number of amplifiers is less than the number of actuators. As a result, it is necessary to restrict the pattern of the switching signals.

The power stage control topology for actuator array used in this paper can save the number of switching elements. Control of each actuator is bi-directional. Conventional design (H-bridge) requires 4 switching elements (e.g., MOSFET) for each actuator. For N actuators, the proposed method requires ($2N$+2) switching elements as compared with $4N$ elements in 1-to-1 cases. In other words, each switching element will be shared by at least two actuators. Therefore, the switching signals to the switching elements cannot be independent. This problem is then formulated as MIMO feedback vector quantization and is solved by the optimization technique proposed in [8]. The proposed method does not restrict the types of reference signals as compared with the one in [9]. Also, the stability analysis of the system is derived to obtain the design conditions. It allows us to design a stable system with arbitrary order. Further, the noise shaping that results in a better tracking of reference signals in the desired bandwidth is achieved by selecting the cut-off frequency of the filter properly.

The paper is organized as follows. Section II introduces the proposed power stage topology and associated control problems. In section III, the MIMO formulation is discussed and the optimal solution is explained. Section IV performs the stability analysis and recommends the conditions that avoid the states of the system exceeding their boundaries. Section V discusses the quantization scheme of the 3-input 3-output system and the sub-optimal concept. Lastly, an example of dual actuators (class-D amplifiers for stereo speakers) is demonstrated. Both cross-talk and SNR results are discussed.

2. POWER AMPLIFIER SCHEME

The architecture of power amplifier used here was discussed in [6]. We present a concise analysis in this section.

2.1 Vector Actuation Power Amplifier

The structure of the actuation system for *N* actuators is shown in Fig. 1. Because switches are shared among adjacent actuators, only *(2N+2)* switches are needed. Comparing to the one-to-one full bridge actuation, the power amplifier used here saves *(2N-2)* switches. Because the actuation commands are not independent among actuators, we discuss the acceptable actuated states in the following.

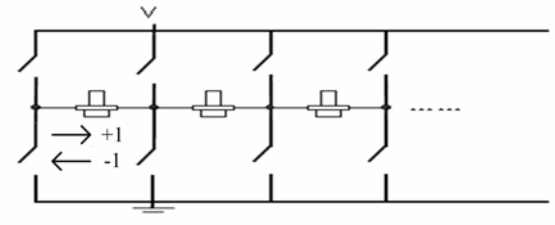

Fig. 1 1x*N* actuator array

2.2 Conditions of 1xn Actuation Power Amplifier

Firstly, the state of zero current is defined as no current flows from the supply voltage side (see Fig.2). Further, let us define the state "1" as current flowing through the actuator to the right direction and "-1" to the left direction (Fig. 1). Two design considerations and the corresponding rules are proposed to obtain the acceptable switching states of the vector actuation power amplifier. First, to protect switching elements from permanent damage, we have to avoid the switching states that result in the short circuit of the system. Second, to prevent the effect caused by mismatching of the actuators, states with sharing of voltage between adjacent actuators are not considered. Therefore, two rules are used when finding the switching conditions of general system [6],

(i) Any two adjacent actuators cannot be in the same state except for zero state.
(ii) Neighborhood actuators next to the zero-state actuator cannot be in the same state except for zero state.

Following the rules, possible states of current flowing direction for dual actuators are shown in Table I. Note that there will be no state like [-1 -1] because it will result in a short circuit (see Fig. 3(a)). By turning off S3 and S4, the dual actuators are put in a serial connection and the voltage drop across each actuator will be 1/2 of the supply voltage if both actuators are identical (see Fig. 3(b)), i.e. yielding the state [1/2 1/2] which violates the rule (i) mentioned above and will not be used.

Now we consider the case of three actuators as indicated in Fig. 4. The acceptable switching conditions for 1×3 actuation system can be calculated by adding an extra actuator at the left side of the dual actuation system which has seven applicable switching states (conditions A to G in Table I). Consequently, the primitive number of switching conditions is $3\times 7=21$. But conditions that violate the rules have to be avoided; the number of acceptable states is less than 21. For example, there are only four acceptable states (conditions E,F,G and H in Table II) when the added actuator of 1×3 actuation system is in state "+1". It is because that state A,B and C in Table II result in the sharing voltage of actuators and state D results in the short circuit of the power stage (see Fig. 5) if the added actuator is in "+1" mode. Note that all of the seven states are allowed if added actuator is in state 0. As a result, the total number of appropriate states is $4+7+4=15=2^4-1$ in 1×3 system.

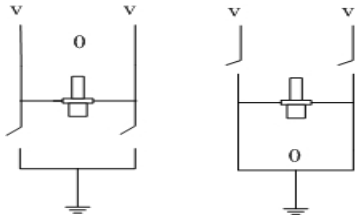

Fig. 2 The switching methods of zero state

Table I Possible states of current flowing direction (L and R represents left and right actuator in Fig. 2)

States	A	B	C	D	E	F	G
L	1	1	0	0	0	-1	-1
R	-1	0	1	0	-1	1	0

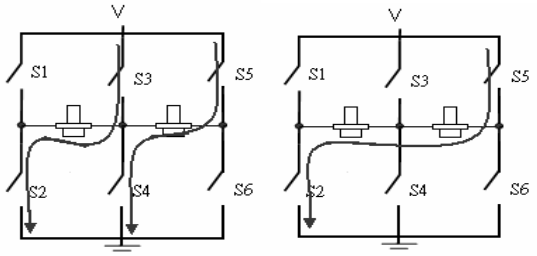

(a) (b)

Fig.3 The switching method of (a) [-1 -1] state which is not allowed because of short circuit (b) [-1/2 -1/2] state

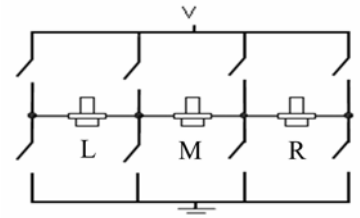

Fig.4 The circuit of 1x3 actuator array

The same procedure can be applied to 4 actuators based on 1×3 system. The number of prohibited states is 0 when added actuator is in "0" state and 7 otherwise. The resulting possible number of states is 31. In general, for *n* actuators, the number of valid states can be shown as [6],

$$3\times(2^{n-1}-1)-2\times(2^{n-2}-1)=2^{n+1}-1. \quad (1)$$

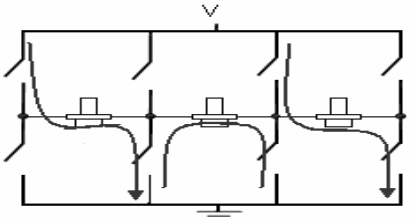

Fig.5 The switching method of [1 0 1] state

Table II some states of 1x3 actuator array

Actuator I	Actuator II	Actuator III	state
1/3	1/3	1/3	A
1/2	1/2	0	B

1/2	1/2	-1	C
1	0	1	D
1	0	0	E
1	0	-1	F
1	-1	1	G
1	-1	0	H
1	-1/2	-1/2	I
-1	0	-1	J
⋮	⋮	⋮	⋮

3. SWITCHING COMMAND GENERATION VIA OPTIMAL FEEDBACK QUANTIZATION

In this section, the method to produce switching commands for general $1\times n$ power stage topology mentioned in preceding section is discussed. The purpose is to track the reference signals. For single actuator, previous work in [10] has proposed a sigma-delta modulation method to generate switching command at a higher sampling rate.

3.1 Optimal MIMO Feedback Quantization

The optimal quantization algorithm proposed in [8] is extended to the MIMO setting as depicted in Fig. 6. The details are introduced in [6] and we only give a brief description. Error vector $\vec{e}$ is the result of difference between up-sampled reference signals $\vec{a}$ and system output $\vec{u}$ filtered by weighting filter *W(z)*. "Optimal Decision Algorithm" computes control forces $\vec{u}_u$ that minimizes $\vec{e}$ and "Quantization" quantizes $\vec{u}_u$ according to the limitation due to the power stage topology as described in Section II (e.g., for dual actuators, there are 7 quantized vector: [1 -1], [1 0], [0 1], [0 -1], [0 0], [-1 1], [-1 0]).

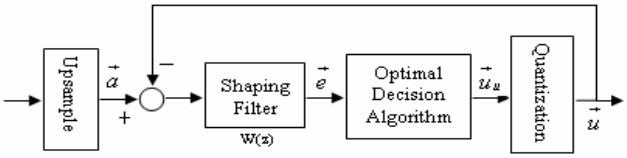

Fig.6 Optimal MIMO Feedback Quantization

$W(z)$ can be represented by a state space form as,

$$\begin{cases}\mathbf{x}(k+1)=A\mathbf{x}(k)+B(\vec{\mathbf{a}}(k)-\vec{\mathbf{u}}(k))\\ \vec{\mathbf{e}}(k)=C\mathbf{x}(k)+D(\vec{\mathbf{a}}(k)-\vec{\mathbf{u}}(k))\end{cases} \quad (2)$$

where $\vec{\mathbf{a}}\in R^{n\times 1}$, $\vec{\mathbf{e}}\in R^{n\times 1}$, $\vec{\mathbf{u}}\in R^{n\times 1}$. n is the dimension of inputs as well as output space. Further, assume the dimension of the state space is $m\times n$, we have $A\in R^{mn\times mn}$, $B\in R^{mn\times n}$, $C\in R^{n\times mn}$, $D\in R^{n\times n}$. The "Optimal Decision Algorithm" is derived by considering the following cost function to minimize $\vec{e}$,

$$V=\vec{\mathbf{e}}(k)^T P\vec{\mathbf{e}}(k) \quad (3)$$

where $P=P^T$ is an $n\times n$ matrix. The optimal solution to the equation above is obtained by substituting (2) into (3), and is,

$$\vec{u}_u=D^{-1}(C\mathbf{x}(k)+D\vec{\mathbf{a}}(k)) \quad (4)$$

The "Quantization" block in Fig. 6 is an *n*-dimensional quantization defined as,

$$\vec{u}=Q^{-1}q\{Q\vec{u}_u\} \quad (5)$$

where $Q^TQ=D^TPD$ and $q\{.\}$ is the Nearest Neighbor Vector Quantizer [8]. The block diagram of "Quantization" is shown in Fig. 7.

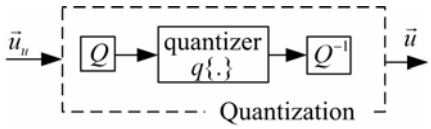

Fig. 7 Block diagram of Quantization

4. BOUNDING THE ERROR SIGNAL AND SYSTEM STATES FOR 1×2 ACTUATOR ARRAY

The stability of the 2-input 2-output nonlinear feedback system (see (2) and (5)) is analyzed based on the idea in [11]. Because the quantization scheme of the optimal feedback system is more complicated than the system in [11], further analysis is required to derive the stability boundary of the allowable input amplitude.

Proposition 1: Consider the 2-input 2-output system (2) under the control law (5) and define $\vec{\mathbf{d}}(k)$ as the input vector of the quantizer (see (4) and (5)). The elements of $\vec{\mathbf{e}}(k)$ are bounded under the zero initial conditions if inputs of the system satisfy,

$\|\vec{\mathbf{a}}(k)\|_\infty\le\bar{a}$, where $\bar{a}=\min(\bar{a}_1,\bar{a}_2)$,

$$\bar{a}_1=\left(\bar{d}_1-\left(|P_{11}(z)|_\infty+|P_{12}(z)|_\infty\right)\bar{e}_1\right)\Big/\left([1\quad 0]Q\begin{bmatrix}1\\1\end{bmatrix}\right),$$

$$\bar{a}_2=\left(\bar{d}_2-\left(|P_{21}(z)|_\infty+|P_{22}(z)|_\infty\right)\bar{e}_1\right)\Big/\left([0\quad 1]Q\begin{bmatrix}1\\1\end{bmatrix}\right)$$

$$\vec{\mathbf{d}}(k)=\begin{bmatrix}d_1(k)\\d_2(k)\end{bmatrix},\ |d_1(k)|_\infty\le\bar{d}_1,\ |d_2(k)|_\infty\le\bar{d}_2,$$

and

$$Z\{C\mathbf{x}(k)\}=\begin{bmatrix}P_{11}(z) & P_{12}(z)\\ P_{21}(z) & P_{22}(z)\end{bmatrix}Z\{\vec{\mathbf{e}}(k)\}.$$

$Z\{y\}$ is the z-transform of y and $\bar{e}_1$ is defined in the proof.

Proof: There are two parts of the proof. First, we show that elements of $\vec{\mathbf{e}}_1(k)\overset{\Delta}{=}QD^{-1}\vec{\mathbf{e}}(k)$ are bounded if the elements of $\vec{\mathbf{d}}(k)$ are bounded. Second, the allowable input amplitude is calculated to prevent elements of $\vec{\mathbf{d}}(k)$ exceeding these bounds.

From (2), (4) and (5), $\vec{\mathbf{e}}(k)$ can be written as,

$$\vec{\mathbf{e}}(k)=C\mathbf{x}(k)+D\vec{\mathbf{a}}(k)-DQ^{-1}q\{QD^{-1}(C\mathbf{x}(k)+D\vec{\mathbf{a}}(k))\} \quad (6)$$

Then we obtain,

$$\begin{aligned}\vec{\mathbf{e}}_1(k)&=QD^{-1}(C\mathbf{x}(k)+D\vec{\mathbf{a}}(k))-q\{QD^{-1}(C\mathbf{x}(k)+D\vec{\mathbf{a}}(k))\}\\ &=\vec{\mathbf{d}}(k)-q\{\vec{\mathbf{d}}(k)\}\end{aligned} \quad (7)$$

Equation (7) indicates that the elements of $\vec{\mathbf{e}}_1(k)$ are the difference between the inputs and the outputs of the Nearest Neighbor Vector Quantizer [8]. Also, for the 2-input 2-output system, this quantizer can be implemented geometrically by computing the nearest distance between the quantizer inputs and the constrained outputs [12]. For example, if only seven of the control commands listed in table1 are considered,

$$U=\left\{\begin{bmatrix}-1\\0\end{bmatrix},\begin{bmatrix}-1\\1\end{bmatrix},\begin{bmatrix}0\\-1\end{bmatrix},\begin{bmatrix}0\\0\end{bmatrix},\begin{bmatrix}0\\1\end{bmatrix},\begin{bmatrix}1\\-1\end{bmatrix},\begin{bmatrix}1\\0\end{bmatrix}\right\}$$

the quantizer output is one of the following vectors,

$$U'=QU$$

$$=\left\{Q\begin{bmatrix}-1\\0\end{bmatrix},Q\begin{bmatrix}-1\\1\end{bmatrix},Q\begin{bmatrix}0\\-1\end{bmatrix},Q\begin{bmatrix}0\\0\end{bmatrix},Q\begin{bmatrix}0\\1\end{bmatrix},Q\begin{bmatrix}1\\-1\end{bmatrix},Q\begin{bmatrix}1\\0\end{bmatrix}\right\}.$$

Hence, one example of the input output relation of the quantizer is shown in Fig. 8 and elements of $\vec{\mathbf{e}}_1(k)$ (i.e. the difference between quantizer inputs and outputs) are bounded if inputs of the quantizer are also bounded [12]. Therefore, we write,

$$\left\|\vec{\mathbf{e}}_1(k)\right\|=\left\|QD^{-1}\vec{\mathbf{e}}(k)\right\|<\bar{e}_1,$$

where $\bar{e}_1$ can be obtained geometrically from Fig. 8 (the derivation is omitted here due to page limit). The bound of $\left\|\vec{\mathbf{e}}(k)\right\|$ is shown below if QD^{-1} is invertible,

$$\left\|\vec{\mathbf{e}}(k)\right\|=\left\|\left(QD^{-1}\right)^{-1}\vec{\mathbf{e}}_1(k)\right\|\le\left\|\left(QD^{-1}\right)^{-1}\right\|\left\|\vec{\mathbf{e}}_1(k)\right\|\le\left\|\left(QD^{-1}\right)^{-1}\right\|\bar{e}_1. \quad (8)$$

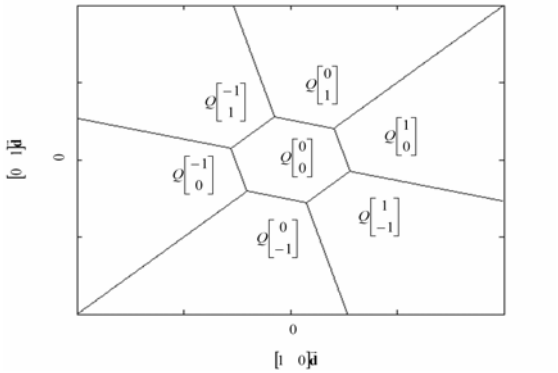

Fig.8 Partition the input space by the quantizer

Secondly, we want to find out the acceptable amplitude of inputs to bound elements of $\vec{\mathbf{d}}(k)$. Because

$d_1(k)=\begin{bmatrix}1 & 0\end{bmatrix}QD^{-1}(C\mathbf{x}(k)+D\vec{\mathbf{a}}(k))$ and

$Z\{C\mathbf{x}(k)\}=\begin{bmatrix}P_{11}(z) & P_{12}(z)\\ P_{21}(z) & P_{22}(z)\end{bmatrix}Z\{\vec{\mathbf{e}}(k)\}$, we obtain

$$Z\{d_1(k)\}=\begin{bmatrix}1 & 0\end{bmatrix}QD^{-1}\begin{bmatrix}P_{11}(z) & P_{12}(z)\\ P_{21}(z) & P_{22}(z)\end{bmatrix}Z\{\vec{\mathbf{e}}(k)\}+\begin{bmatrix}1 & 0\end{bmatrix}QZ\{\vec{\mathbf{a}}(k)\}$$

If the bound is set as,

$$\left|d_1(k)\right|_\infty\le\bar{d}_1 \quad (9)$$

the amplitude of inputs must satisfy the following equation to prevent violation of (9) under the zero initial conditions [11],

$$\left\|\vec{\mathbf{a}}(k)\right\|_\infty\le\left(\bar{d}_1-\left\|QD^{-1}\right\|\left(\left|P_{11}(z)\right|_\infty+\left|P_{12}(z)\right|_\infty\right)\left\|\left(QD^{-1}\right)^{-1}\right\|\bar{e}_1\right)\Big/\left(\begin{bmatrix}1 & 0\end{bmatrix}Q\begin{bmatrix}1\\1\end{bmatrix}\right) \quad (10)$$

The same procedure is applied to the limit,

$$\left|d_2(k)\right|_\infty\le\bar{d}_2$$

and the allowable input amplitude is,

$$\left\|\vec{\mathbf{a}}(k)\right\|_\infty\le\left(\bar{d}_2-\left\|QD^{-1}\right\|\left(\left|P_{21}(z)\right|_\infty+\left|P_{22}(z)\right|_\infty\right)\left\|\left(QD^{-1}\right)^{-1}\right\|\bar{e}_1\right)\Big/\left(\begin{bmatrix}0 & 1\end{bmatrix}Q\begin{bmatrix}1\\1\end{bmatrix}\right) \quad (11)$$

As a result, the amplitude of inputs must satisfy both (10) and (11) as indicated in proposition 1.

Proposition 2: For the 2-input 2-output system (2) under the control law (5), the states are bounded under the zero initial conditions if

(i) zeros of the system $W(z)$ are stable

(ii) elements of $\left\|\vec{\mathbf{e}}(k)\right\|$ are bounded

Proof: From (2), $\vec{\mathbf{u}}(k)$ is written as,

$$\vec{\mathbf{u}}(k)=\vec{\mathbf{a}}(k)-D^{-1}(\vec{\mathbf{e}}(k)-C\mathbf{x}(k)) \quad (12)$$

Substituting (12) into the first equation of (2), the system is then become,

$$\mathbf{x}(k+1)=(A-BD^{-1}C)\mathbf{x}(k)+BD^{-1}\vec{\mathbf{e}}(k) \quad (13)$$

If elements of $\vec{\mathbf{e}}(k)$ are bounded, then the states are bounded if the system (13) is stable, indicating that the eigenvalues of the matrix $\left(A-BD^{-1}C\right)$ must lie inside the unit circle. If the shaping filter $W(z)$ is designed without pole zero cancellation, then the eigenvalues of $\left(A-BD^{-1}C\right)$ are exactly the zeros of $W(z)$ [11]. Therefore, the system with stable zeros has bounded states under zero initial conditions if the amplitude of both inputs satisfies (10) and (11).

For general $1\times n$ actuation systems, the same procedure can be applied to ensure the stability of the system under zero initial conditions. The key idea is that we have to select the upper bound of the quantizer inputs and find out the maximum difference between inputs and outputs of the quantizer (see (7)). Once the elements of $\vec{\mathbf{e}}_1(k)$ are all bounded, the error is also bounded (see (8)) indicating that the states of system with stable zeros are all bounded if the amplitude of inputs is limited by,

$$\left\|\vec{\mathbf{a}}(k)\right\|_\infty\le\min(a_1,a_2,\cdots a_n)$$

where $$a_i\le\left(\bar{d}_i(k)-\left\|QD^{-1}\right\|\left\|\left(QD^{-1}\right)^{-1}\right\|\left(\sum_{k=1}^{n}\left|P_{ik}(z)\right|_\infty\right)\bar{e}_i\right)\Big/\left(\begin{bmatrix}0 & 1\end{bmatrix}Q\begin{bmatrix}1\\1\end{bmatrix}\right)$$

and $\bar{d}_i(k)$ is the upper bound of the i-th input of the quantizer. To obtain the bound of $\vec{\mathbf{e}}_1(k)$ (see (7)), the analysis of optimal quantization scheme is required. In the following, the quantization system with 3 actuators is discussed.

5. QUANTIZATION SHCEME OF THE 3-ACTUATOR SYSTEM

For 1×3 actuation system (see Fig.4), there are 15 situations can be selected for the quantizer output (see (1)). Because the input of the quantizer is a vector with length 3, the quantization partitions the 3-D space into 15 portions according to nearest distance between input and constrained output of the quantizer. Although it can also be solved geometrically, the cost of implementation is high due to the complexity. Therefore, a suboptimal architecture of the quantization is proposed here to reduce the dimension of the quantizer (see Fig.9), i.e., the 3-dimensional quantization is replaced by a 2-dimension quantizer (see Fig. 8) and a one-dimension quantizer (scalar quantizer). Inputs of 2-dimensional quantizer are selected from the first or the last two inputs of quantization block and the input of the other quantizer is the remainder one. Because these three outputs of the quantization are not independent, the results of 2-dimensional quantization will influence the output of the 1-dimensional quantization. In the implementation, the outputs of 2-dimensional quantizer are calculated first and then the

results are used to calculate the output of 1-dimensional quantizer. As a result, the error of the remainder channel is larger than the other two. To avoid this phenomenon, the inputs of 2-dimension quantizer will be selected alternatively from the first and the last two inputs of the quantization block.

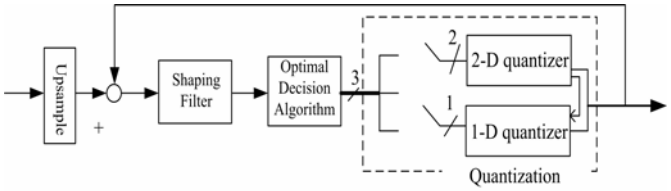

Fig. 9 Block diagram of the system with sub-optimal quantization

6. EXAMPLE AND SIMULATION RESULT

The architecture proposed in this paper is applied to dual-channel class-D audio amplifier. In the traditional class-D amplification, half-bridge and full-bridge power amplifier are usually used. Comparing to the half-bridge, the system in this paper avoids the circuit to produce mid-voltage that influences the performance seriously. Further, the system protects 2 switching devices as compared to full-bridge system in dual-channel actuation. In the following, the design of the shaping filter and 2-D quantizer are discussed with calculating the maximum input amplitude for stability. The simulation in second part verifies the performance and stability boundaries of the system.

6.1 Design Example

Since there is no coupling of the actuators and both actuators are identical, the weighting filter $W(z)$ can be written as:

$$W(z)=\begin{bmatrix} w_{11}(z) & w_{12}(z) \\ w_{21}(z) & w_{22}(z) \end{bmatrix}=\begin{bmatrix} w(z) & 0 \\ 0 & w(z) \end{bmatrix}$$

Because the bandwidth of input audio signal is within 22.05kHz, the performance is characterized at low frequency. Therefore, $w(z)$ is selected as a second order low-pass filter with cutoff frequency 150kHz. The state space matrices of the system are:

$$A=\begin{bmatrix} 0 & -1 & 0 & 0 \\ 1 & 2 & 0 & 0 \\ 0 & 0 & 0 & -1 \\ 0 & 0 & 1 & 2 \end{bmatrix}, B=\begin{bmatrix} -0.44 & 0 \\ 0.53 & 0 \\ 0 & -0.44 \\ 0 & 0.53 \end{bmatrix}, C=\begin{bmatrix} 0 & 1 & 0 & 0 \\ 0 & 0 & 0 & 1 \end{bmatrix}, D=\begin{bmatrix} 1.24 & 0 \\ 0 & 1.24 \end{bmatrix}$$

Because the eigenvalues of $\left(A-BD^{-1}C\right)$ are $(0.79\pm j0.18)^2$, the zeros of the system are stable. Further, by selecting $P=\begin{bmatrix} 1 & 0.5 \\ 0.5 & 1 \end{bmatrix}$ and using singular value decomposition, we get $Q=\begin{bmatrix} -0.62 & 0.62 \\ 1.08 & 1.08 \end{bmatrix}$. To avoid the mismatch of speakers, we use only seven of the control commands listed in table 1:

$$U=\left\{\begin{bmatrix} -1 \\ 0 \end{bmatrix},\begin{bmatrix} -1 \\ 1 \end{bmatrix},\begin{bmatrix} 0 \\ -1 \end{bmatrix},\begin{bmatrix} 0 \\ 0 \end{bmatrix},\begin{bmatrix} 0 \\ 1 \end{bmatrix},\begin{bmatrix} 1 \\ -1 \end{bmatrix},\begin{bmatrix} 1 \\ 0 \end{bmatrix}\right\}$$

Therefore, the quantizer partitions its 2-dimensional input space into seven regions according to the nearest neighbor rule. Since

$$U'=QU=$$

$$\left\{\begin{bmatrix} -0.62 \\ 1.08 \end{bmatrix},\begin{bmatrix} -1.24 \\ 0 \end{bmatrix},\begin{bmatrix} 0 \\ 0 \end{bmatrix},\begin{bmatrix} -0.62 \\ -1.08 \end{bmatrix},\begin{bmatrix} 0.62 \\ 1.08 \end{bmatrix},\begin{bmatrix} 0.62 \\ -1.08 \end{bmatrix},\begin{bmatrix} 1.24 \\ 0 \end{bmatrix}\right\},$$

the partitions are obtained by computing the nearest point in U'. Hence, the input output relation of the quantizer is shown in Fig. 10. To ensure the stability of the system, the amplitude of inputs are limited to,

$$\left\|\vec{\mathbf{a}}(k)\right\|_\infty \le \bar{a}=\min(0.32,0.38)=0.32\,.$$

And the boundaries of inputs of the quantizer are,

$$\left\|d_1(k)\right\|_\infty \le 1.24,\ \left\|d_2(k)\right\|_\infty \le 1.79\,. \qquad (14)$$

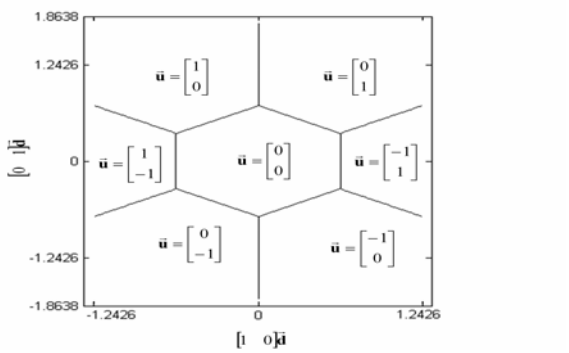

Fig.10 Partition the input space by the quantizer

To compute the output $\vec{u}=(u_1\ \ u_2)^T$, a straightforward method is to construct the quantization boundary. For example, Fig. 11 shows the geometrical partitions of u_1 where the boundaries can be described as,

$$v_1 = sign\{-x+1.73y\}+sign\{-x+0.62\}$$
$$\quad +sign\{-x+1.73y+1.24\}+sign\{-x\}$$
$$v_2 = sign\{-x+1.73y\}+sign\{-x-0.62\}$$
$$\quad +sign\{-x+1.73y-1.24\}+sign\{-x\}$$

where

$$sign(y)=\begin{cases} 1 & if\ \ y>0 \\ 0 & if\ \ y=0 \\ -1 & if\ \ y<0 \end{cases}$$

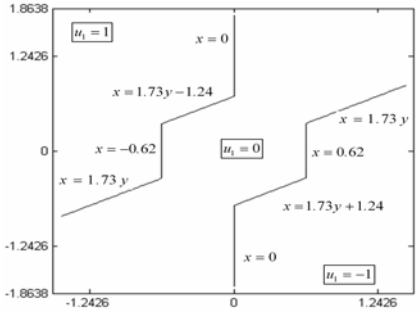

Fig.11 input output relation of the quantized variable u_1

It can be shown that,

$$u_1=\begin{cases} sign(v_1) & for\ \ sign(v_1)=sign(v_2) \\ 0 & else \end{cases}.$$

The second element u_2 can be obtained in the same way.

6.2 Simulation Results

Two sinusoidal waves at 1 KHz and 2 KHz with normalized amplitude 0.3 and sampled at 48 KHz are applied to the

system as the reference signals. Fig.12 and Fig. 13 plot the output spectrum obtained by taking DFT (Discrete Fourier Transform) of the binary outputs. The resulting SNDR (Signal to Noise Distortion Ratio, see [10]) are 97dB and 98dB respectively. SNDR already characterizes the cross-talk by viewing its negative values (e.g., -97 dB and -98 dB). Specifically, it can be seen from Fig. 12 that the amplitude of 2 KHz signal is 97 dB below the reference signal at 1 KHz. The same result can be observed from Fig.13. Fig.14 shows the resulting output waveforms filtered by a low pass filter cutoff at 22.05 KHz. Fig. 15 plots the inputs of the quantizer which satisfy (14).

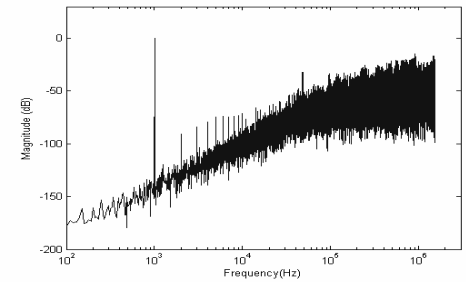

Fig.12 DFT of output1

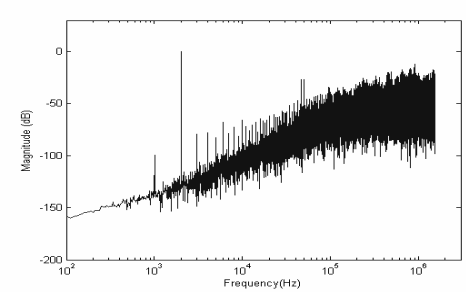

Fig.13 DFT of output2

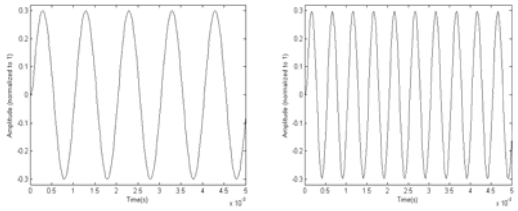

(a) (b)

Fig.14 Waveform of output1 after filtering (a)1 KHz (b) 2 KHz

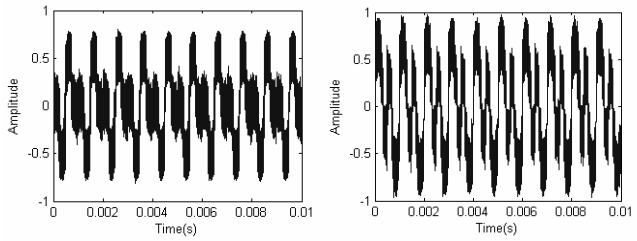

(a) (b)

Fig 15. Inputs of quantizer $\vec{\mathbf{d}}(k)$ (a) $d_1(k)$ (b) $d_2(k)$

7. CONCLUSION

The vector actuated power amplification using MIMO optimal feedback quantization is analyzed here. The architecture of power amplification saves *(2N-2)* switching devices comparing to the independent full-bridge actuation system. The stability analysis of MIMO optimal feedback quantization is proposed basing on bounding the system states. Further, the states can be bounded by limiting the maximum amplitude of inputs if the zeros of the shaping filter are all stable. The architecture of 3-D quantizer in 1×3 actuation system is addressed considering the sub-optimal solution of the cost function. It shows that the 3-dimension quantization can be replaced by a 2-D quanitzer and a scalar quantizer connected in serial. In the example, a stable 2-input 2-output system which is applied to dual-channel class-D audio amplifier is designed. The simulation results show the effectiveness of the proposed scheme in both control performance and very little cross-talk. In the future work, the quantization scheme of general $1\times n$ system will be derived considering the sub-optimal of the cost function. This method simplifies the implementation of quantization block efficiently.

ACKNOWLEDGMENT

This work was supported by National Science Council of the R.O.C. under grant no. NSC94－2218－E009064 and MOE ATU Program under the account number 95W803E.

REFERENCES

[1] Leslie Flemming and Stephen Mascaro, “Control of Scalable Wet SMA Actuator Arrays,” Proceedings of the 2005 IEEE International Conference on Robotics and Automation, Barcelona, Spain, April 2005.

[2] Thomas G. Bifano et al., ”Continuous-membrane Surface-micromachined Silicon Deformable Mirror,” Opt. Eng. 36(5) 1354–1360 (May 1997).

[3] Gunter Stein and Dimitry Gorinevsky, “Design of Surface Shape Control for Large Two-Dimensional Arrays, IEEE Transactions On Control Systems Technology, Vol. 13, No. 3, May 2005.

[4] Christopher Frauenberger and Markus Noisternig, “3D Audio Interfaces for the Blind,” Proceedings of the 2003 International Conference on Auditory Display, Boston, MA, USA, July 6-9, 2003.

[5] http://www.holosonics.com/technology.html

[6] Jwu-Sheng Hu and Keng-Yuan Chen, " A Novel Switch Mode Amplifier Design for Actuator Array Using MIMO Optimal Feedback Quantization," 2007 American Control Conference, New York, USA. July 11-13, 2007.

[7] Kyu-Jin Cho, Samuel Au, H. Harry Asada, “Large-scale Control Using a Matrix Wire Network for Driving a Large Number of Actuators,” In Proceedings of the 2003 IEEE, International Conference on Robotics & Automation, Taipei, Taiwan, September 14-19

[8] Daniel E. Quevedo, Graham C. Goodwin,”Audio Quantization from a Receding Horizon Control Perspective,” Proceedings of the American Control Conference, Denver, Colorado June 4-6,2003

[9] Kyu Min Cho, Won Seok Oh, Won Sup Chung, Hee Jun Kim,”A New Class-D Stereo Audio Amplifier Using Direct Speaker Current Control” 2004 35th Annual IEEE Power Electronics Specialists Conference.

[10] Jwu-Sheng Hu and Keng-Yuan Chen, “Implementation of a Full Digital Amplifier Using Feedback Quantization,” 2006 American Control Conference, Minneapolis, Minnesota USA. June 14-16, 2006.

[11] Shiang-Hwua Yu, “Noise-Shaping Coding Through Bounding the Frequency-Weighted Reconstruction Error,” IEEE Transactions On Circuit And Systems I: Express Briefs, VOL. 53, NO. 1, JANUARY 2006

[12] Jwu-Sheng Hu and Keng-Yuan Chen, "An FPGA Implementation Of Finite Horizon Constrained Optimization For A Full Digital Amplifier," 2007 American Control Conference, New York, USA. July 11-13, 2007.